HHS Public Access

Author manuscript

IEEE J Biomed Health Inform. Author manuscript; available in PMC 2020 July 01.

Published in final edited form as:

IEEE J Biomed Health Inform. 2019 July ; 23(4): 1516–1525. doi:10.1109/JBHI.2018.2871141.

Template-Based Statistical Modeling and Synthesis for Noise Analysis of Ballistocardiogram Signals: A Cycle-Averaged Approach

A. Ozan Bicen [Member, IEEE], **Daniel C. Whittingslow**, **Omer T. Inan [Senior Member, IEEE]**

School of Electrical and Computer Engineering, Georgia Institute of Technology, Atlanta, GA 30332

Abstract

Objective: Ballistocardiogram (BCG) can be recorded using inexpensive and non-invasive hardware to estimate physiological changes in the heart. In this work, a methodology is developed to evaluate the impact of additive noise on the BCG signal.

Methods: A statistical model is built that incorporates subject-specific BCG morphology. BCG signals segmented by ECG RR intervals (BCG heartbeats) are averaged to estimate a parent template and sub-templates leveraging the quasi-periodic nature of the heart. Noise statistics are obtained for sub-templates with respect to the parent template. Then, a synthesis algorithm with adjustable additive noise is devised to generate sub-templates based on the individual's parent template and statistics. For the example use of the synthesis algorithm, the average correlation coefficient between sub-templates and the parent template (sub-template versus parent template approach) is tested as a signal quality index (SQI).

Results: A BCG heartbeat synthesis framework that incorporates an individual's BCG morphology, and physiological variability was developed to quantify variations in the BCG signal against additive noise. The signal quality assessment of a person's BCG recording could be performed without requiring any a priori knowledge on the person's BCG morphology. A data-driven constraint on the required minimum number of heartbeats for the reliable template estimation was provided.

Conclusion: The impact of additive noise on BCG morphology and estimated physiological parameters can be analyzed using the developed methodology without requiring prior statistics.

Significance: This work can facilitate performance evaluation of BCG analysis algorithms against additive noise.

Keywords

Ballistocardiogram; cardiovascular sensing; matched filtering; noise analysis; precision medicine; statistical modeling; template estimation

bozan@ece.gatech.edu.

1. Introduction

THE ever increasing burden of cardiovascular disease (CVD) can be mitigated using the recent advances in cardiovascular sensing systems that can facilitate proactive monitoring and personalization of care [1], [2]. A promising sensing methodology is the combination of the ballistocardiogram (BCG) and the electrocardiogram (ECG), from which the changes in the heart's functioning can be estimated [3]–[6].

BCG signals can be recorded using non-invasive, easy-to-use, and low-cost hardware such as a modified weighing scale [7]–[10]. While BCG acquisition from a weighing scale may facilitate home monitoring of the variations in the cardiovascular system, the method is susceptible to various sources of noise. BCG signal morphology is greatly variable, which can be due to subject-specific (personal) cardiovascular or respiratory system differences, as well as external noise. External noise involves any noise generated outside of the functioning of the cardiopulmonary system, e.g., motion artifacts and instrumentation noise. External noise may be sufficiently large that it can distort the BCG morphology and reduce the *reliability* of the estimated cardiovascular system parameters. Here, the reliability refers to the accuracy and repeatability of the estimated parameters from the BCG. To the best of our knowledge, there is no prior work that addresses modeling, synthesis, and quantification of noise for BCG signals. The development of a computational prototype that can enable performance evaluation of BCG feature extraction and parameter estimation algorithms with respect to noise has been an open problem.

In this work, our objective is to develop a statistical model and devise a synthesis algorithm to assess the sensitivity of an individual's BCG morphology to additive noise. The statistical model leverages the underlying quasi-periodic nature of the cardiopulmonary system with the aid of ECG RR intervals to estimate template BCG heartbeats and statistics. The synthesis algorithm uses the developed statistical model and incorporates an additive noise component with adjustable statistical properties. The overall synthesis framework can facilitate prediction of the reliability of the estimated cardiovascular parameters from BCG by means of creating random realizations of BCG heartbeats distorted by the additive noise. To show an example use of the developed model and synthesis algorithm, we propose a BCG signal quality index (SQI) based on matched filtering and estimated template BCG heartbeats to detect BCG recordings corrupted by additive noise.

II Signal Description and Abstraction

The BCG is a measurement of the movements of the body in response to the heartbeat, specifically, the mechanical recoil of the body against the ejected blood by the heart into the vascular system [3]. The BCG signal can be acquired based on the vertical displacements of a body weighing platform against gravity, while the person stands upright (Fig. 1(a)). The ECG is a measurement of cardiac electrophysiology [11]. The ECG signal can be acquired using gel or handlebar electrodes held by the person while standing on the weighing platform.

We use the conventional pre-processing of the BCG signals utilizing the ECG RR intervals as a repeating cycles in each heartbeat [12]. Pre-processing of the BCG signal recorded over a period of time is done in two steps. The first step is the segmentation of the BCG signal into "heartbeats" based on the ECG RR interval (see Fig. 1(b), (c), and (d)). In this paper, we refer to BCG signal segments between each ECG RR interval as *BCG heartbeats*. The second step of pre-processing is the averaging of the each sample in BCG heartbeats over a constant number of consecutive RR intervals (see Fig. 1(e), and (f)). We denote the averaged BCG heartbeats across RR intervals as *cycle-averaged* BCG heartbeats. The data-driven cycle averaging process preserves the dependence of the estimated template on the subject-specific (personal) BCG morphology. This is a fundamental advantage over the *a priori* determination of such properties of the signal during model development [13], [14]. Cycle-averaged BCG heartbeats form the basis of our proposed template estimation for the statistical modeling and synthesis of BCG signals.

The cycle-averaged BCG heartbeat is modeled incorporating the statistics of the additive noise and the electro-mechanical delay (RJ interval). To this end, a parent template (pseudotrue) BCG heartbeat is estimated for each subject using *all* the heartbeats in the individual's recordings (see Fig. 1(f)). We also compute sub-templates using only a *subset* of the BCG heartbeats during cycle-averaging (see Fig. 1(e)). Utilizing the developed statistical model, an algorithm is devised for synthesis of cycle-averaged BCG heartbeats, where synthetic additive noise is generated based on the estimated statistics with an adjustable gain. To the best of our knowledge, this is the first attempt to develop a data-driven and synthesis framework for BCG signals, which is an essential task to quantify the reliability of the estimated health parameters. Additionally, we introduce a BCG SQI based on the average of the correlation coefficient between the sub-templates and the parent template BCG heartbeat (sub-template versus parent template approach), which can quantify the reliability of BCG signals recorded outside of controlled environments.

III. Template Estimation

A. BCG Heartbeat Extraction between RR Intervals

The BCG heartbeat $\mathbf{c}_n$ for each R-peak n is obtained by dividing the recorded BCG signal into equal length segments with respect to the ECG R-peaks. Each consecutive R-peak marks the beginning of the BCG heartbeat. The minimum RR interval in the ECG recording for a human subject gives the segment size T_{RR}. For a sampling rate, f_s, the length (L) of the BCG heartbeat vector ($\mathbf{c}_n$) is $L = T_{\mathrm{RR}} f_s$. The vector $\mathbf{c}_n$ is defined as $c_n = \left[c_n^{(1)}, c_n^{(2)}, \cdots, c_n^{(L)}\right]^{\mathrm{T}}$. The total number of RR intervals in the BCG signal recording is N. Example BCG heartbeats are illustrated in Fig. 1(d).

B. Parent Template and Sub-Template BCG Heartbeats

For statistical modeling of the additive noise and the RJ interval, we denote the sample mean of the BCG heartbeats in the BCG recording as the pseudo-true value of the parent template BCG heartbeat (In the literature, the parent template BCG heartbeat is also often referred to as an "ensemble averaged" BCG). The parent template BCG heartbeat, ψ, is estimated over all RR intervals, N, as

$$\widehat{\psi} = \frac{1}{N}\sum_{n=1}^{N} \boldsymbol{c}_n, \quad (1)$$

where $\widehat{\psi} = \left[\psi^{(1)}, \cdots, \psi^{(L)}\right]^{\mathrm{T}}$. An example parent template BCG heartbeat is illustrated in Fig. 1(f). The RJ interval for the parent template BCG heartbeat, $\tau_{\psi}^{\mathrm{RJ}}$, is estimated as

$$\widehat{\tau}_{\psi}^{\mathrm{RJ}} = \arg \max_{l/f_s \in [0.1, 0.35]} \widehat{\psi}, \quad (2)$$

where l is the discrete-time index, and f_s is the sampling rate of the instrumentation system. The peak of the BCG's J-wave was searched for between 0.1sec and 0.35sec of the parent template BCG heartbeat.

Several factors can affect the cardiovascular system (e.g., respiration, physical activity, and mental stress), and hence, the RJ interval is not constant from beat-to-beat but rather varies throughout a given BCG recording. In our model, we assume that measurements are taken at rest while the subject is standing upright and not moving. To mitigate the beat-to-beat RJ interval variability, rather than analyzing the BCG heartbeats individually on a *beat-by-beat* basis, we analyze averaged BCG heartbeats over a limited number of RR intervals, W, that is smaller than the total number of RR intervals, N. These averaged heartbeats are used to estimate sub-templates for a given BCG recording.

To obtain the RJ interval and additive noise statistics, we exploit sub-template BCG heartbeats $\mathbf{s}_q$, where q is the subtemplate index. Each sub-template is composed of W adjacent BCG heartbeats. Example BCG heartbeat sub-templates are illustrated in Fig. 1(d). The number of sub-templates is given by $\eta = \lfloor N/W \rfloor$. The sub-template, $\mathbf{s}_q$, is estimated by the sample mean of W adjacent BCG heartbeats as

$$\widehat{s}_q = \frac{1}{W}\sum_{n=(q-1)W+1}^{qW} \boldsymbol{c}_n, \quad (3)$$

where $\widehat{s}_q = \left[s_q^{(1)}, \cdots, s_q^{(L)}\right]^{\mathrm{T}}$. $\widehat{\mathbf{s}}_q$ will be used to obtain the RJ interval and additive noise statistics with respect to $\widehat{\psi}$.

IV. Statistical Modeling

A. Signal Model

Based on the parent template and sub-template BCG heartbeats defined in Section III-B, the following signal model is considered

$$\begin{aligned} \mathrm{s} &= \left(\psi + \mathbf{w}_{\mathrm{phy}}\right) * \delta\left(t - \nu^{\mathrm{RJ}}\right) + \mathbf{w}_{\mathrm{ext}} \\ &= \psi\left(t - \nu^{\mathrm{RJ}}\right) + \mathbf{w}, \end{aligned} \quad (4)$$

where **s** is the sub-template BCG heartbeat, ψ is the parent template BCG heartbeat, $\mathbf{w}_{\mathrm{phy}}$ is the physiological variability, $\mathbf{w}_{\mathrm{ext}}$ is the external noise, * is the convolution operator, δ is the Dirac delta function, t is the time index $\left(t = l/f_s\right)$, ν^{RJ} is the jitter of the RJ interval, and **w** represents the total additive noise composed of both random physiological variations and external noise as $\mathbf{w} = \mathbf{w}_{\mathrm{phy}}\left(t - \nu^{\mathrm{RJ}}\right) + \mathbf{w}_{\mathrm{ext}}$. $\mathbf{w}_{\mathrm{phy}}$ is a physiological feature and corresponds to the variations in the BCG signal due to the normal cardiac variability over time [18]–[20]. The ν^{RJ} term captures the physiological variation that occurs during the cardiac signal transduction and mechanical valve operation [18]–[20]. $\mathbf{w}_{\mathrm{ext}}$ represents the external noise which captures the motion artifacts and instrumentation noise. Addition of $\mathbf{w}_{\mathrm{phy}}$ and $\mathbf{w}_{\mathrm{ext}}$ terms are denoted as the additive noise **w** in this work. Overall, **s** is shifted by random delay ν^{RJ} and altered by additive noise **w**. For discrete-time calculations, time index, t, is converted to sample index, l, using the sampling rate, f_s, i.e., $l = tf_s$, and the Dirac delta function is replaced with the Kronecker delta function.

Next, we present the statistics of the RJ interval jitter, ν^{RJ}, and additive noise, **w**, using the estimated template and subtemplate heartbeats.

B. Statistics of the RJ Interval Jitter

The RJ interval for the sub-templates is shifted by a random phase with respect to the template BCG. For example, in Fig. 1 (c), variation of the RJ intervals among 6-beat averaged BCG heartbeats can be observed. This random jitter is estimated for each sub-template as

$$\hat{\nu}_q^{\mathrm{RJ}} = \hat{\tau}_{\mathrm{s}_q}^{\mathrm{RJ}} - \hat{\tau}_{\psi}^{\mathrm{RJ}}, \quad (5)$$

where the RJ interval for each estimated sub-template BCG heartbeat is given by

$$\hat{\tau}_{\mathrm{s}_q}^{\mathrm{RJ}} = \arg \max_{l/f_s \in [0.1, 0.35]} \hat{\mathbf{s}}_q, \quad (6)$$

where the peak of the BCG's J-wave was searched for between 0.1sec and 0.35sec of each sub-template BCG heartbeat. The sample mean of the RJ interval random delay is obtained as

$$\hat{\mu}_{\nu^{\mathrm{RJ}}} = \frac{1}{\eta} \sum_{q=1}^{\eta} \hat{\tau}_{\mathrm{s}_q}^{\mathrm{RJ}} - \hat{\tau}_{\psi}^{\mathrm{RJ}}. \quad (7)$$

The sample variance of the RJ interval random delay is computed as

$$\hat{\sigma}^2_{\nu^{\mathrm{RJ}}} = \frac{1}{\eta - 1} \sum_{q=1}^{\eta} \left(\left(\hat{\tau}^{\mathrm{RJ}}_{s_q} - \hat{\tau}^{\mathrm{RJ}}_{\psi} \right) - \hat{\mu}_{\nu^{\mathrm{RJ}}} \right)^2 . \quad (8)$$

C. Statistics of the Additive Noise

We study additive noise with two methods: 1) the additive noise statistics for sub-template BCG heartbeats, and 2) the average noise power across the sub-template heartbeats.

1) Additive Noise Level in Sub-Template BCG Heartbeats: Additive noise in the sub-template BCG heartbeats $\widehat{\mathbf{w}}_q$ is estimated across the sub-template heartbeats as

$$\widehat{\mathbf{w}}_q = \hat{\mathbf{s}}_q \left(t + \nu^{\mathrm{RJ}}_q \right) - \hat{\psi} . \quad (9)$$

The sample mean of the additive noise $\hat{\mu}_{\mathbf{w}}$ is estimated across the sub-template heartbeats as

$$\hat{\mu}_{\mathbf{w}} = \frac{1}{\eta} \sum_{q=1}^{\eta} \hat{\mathbf{s}}_q \left(t + \nu^{\mathrm{RJ}}_q \right) - \hat{\psi} . \quad (10)$$

The sample variance of the additive noise $\hat{\sigma}^2_{\mathbf{w}}$ is estimated across the sub-template heartbeats as

$$\hat{\sigma}^2_{\mathrm{W}} = \mathrm{diag} \left(\frac{1}{\eta - 1} \sum_{q=1}^{\eta} \left(\widehat{\mathbf{w}}_q - \hat{\mu}_{\mathbf{w}} \right)^{\mathrm{T}} \left(\widehat{\mathbf{w}}_q - \hat{\mu}_{\mathbf{w}} \right) \right). \quad (11)$$

2) Average Noise Power of Sub-Template BCG Heartbeats: Average noise power for the qth sub-template BCG heartbeat is given by

$$\hat{\lambda}_q = \frac{1}{L} \left(\widehat{\mathbf{w}}_q - \hat{\zeta}_{\mathbf{w}_q} \right)^T \left(\widehat{\mathbf{w}}_q - \hat{\zeta}_{\mathbf{w}_q} \right), \quad (12)$$

where L is the length of additive noise vector $\mathbf{w}$, and $\hat{\zeta}_{\mathbf{w}_q}$ is calculated as

$$\hat{\zeta}_{\mathbf{w}_q} = \frac{1}{L} \sum_{l=1}^{L} \widehat{\mathbf{w}}^{(l)}_q . \quad (13)$$

V. Template-Based Synthesis and Matched Filtering for Noise Analysis

A. Sub-Template BCG Heartbeat Synthesis Algorithm

The block diagram of the sub-template BCG heartbeat synthesis algorithm is given in Fig. 2. The algorithm performs the following steps:

1. Template and sub-template BCG heartbeats are estimated as described in Section III-B. Then, RJ interval and additive noise statistics are obtained as described in Section IV-B and IV-C. Each point l in the additive noise vector $\mathbf{w}$ of a sub-template BCG heartbeat is created using the estimated mean and variance in (10) and (11), respectively, where each point l is taken to be independent and normally distributed. Power of the randomly generated additive noise vector during synthesis of the sub-template is normalized to unit norm (normalized sub-template noise).
2. Noise power per sub-template BCG heartbeat is created using the noise power obtained in (12). Then, noise power for each sub-template BCG heartbeat is scaled with the adjustable noise gain. This noise gain can be a scalar as well as a coloring transformation for correlated power scaling of additive noise. Power-scaled additive noise is passed through a standard bandpass filter (0.8–20Hz) used for BCG signal processing [16], [17], and added to the replicated parent template BCG heartbeats toward synthesis of sub-template BCG heartbeats.
3. RJ intervals for each sub-template BCG heartbeat are randomly generated based on the statistics obtained in (7) and (8), and using independent normally distributed random variables. Lastly, the noise added sub-template BCG heartbeats are shifted based on the jitter of the RJ intervals.

The developed noisy sub-template BCG heartbeat generation algorithm reflects a data-driven approach for modeling of the electro-mechanical activity of the heart. This model can provide a valuable tool for testing robustness of feature extraction algorithms applied to BCG signals with different measurement durations, noise levels, and sampling frequencies. For example, synthetic noise can be generated with different power levels and autocorrelations to study the *misdetection* and *false-alarm* probabilities of a given technique.

B. Noise Analysis for BCG Signal Quality Assessment

We propose the average linear correlation coefficient (the sample mean of the linear correlation coefficient) between the sub-templates and the parent template BCG signal for the quantification of the noisiness (quality) of the BCG signal. The parent template is expected to be correlated to the sub-templates, since the parent template is computed as the average of the sub-templates. Assuming the subject is standing upright without moving, respiration rate is expected to be a component of the system that may modulate the cardiac function in a BCG recording (there are approximately 3–8 heartbeats in a complete breathing cycle, and an increase in the rate or depth of ventilation promotes ventricular SV [18], [21] which affects BCG morphology). Therefore, it is also physiologically expected that the sub-templates should be correlated to the parent template. We calculate the Pearson

correlation coefficient between the parent template and sub-templates analogously as in a correlation receiver (matched filter) case [22].

The average correlation coefficient (ρ) is calculated over all of the sub-templates in a recording as

$$\rho = \frac{1}{\eta}\sum_{q=1}^{\eta} \frac{\left(\psi - \mu_\psi\right)^{\mathrm{T}}\left(\mathrm{s}_q - \mu_\psi\right)}{\sqrt{\left(\psi - \mu_\psi\right)^{\mathrm{T}}\left(\psi - \mu_\psi\right)}\sqrt{\left(\mathrm{s}_q - \mu_{\mathrm{s}_q}\right)^{\mathrm{T}}\left(\mathrm{s}_q - \mu_{\mathrm{s}_q}\right)}}, \quad (14)$$

where $\mu_\psi = E\left\{\psi^{(l)}\right\}$ is the sample-by-sample average of ψ as $\mu_\psi = \frac{1}{L}\sum_{l=1}^{L}\psi^{(l)}$ and $\mu_{\mathrm{s}_q} = E\left\{s_q^{(l)}\right\}$ is the sample-by-sample average of the s_q as $\mu_{\mathrm{s}_q} = \frac{1}{L}\sum_{l=1}^{L}s_q^{(l)}$.

Calculation of (14) does not depend on any prior knowledge (side information) of the BCG signal, since the parent template BCG heartbeat and sub-templates are calculated in an online manner with the arrival of the BCG and ECG recordings. Simultaneously recorded BCG and ECG measurements can be pre-processed as described in Section III to obtain the parent template and sub-templates, then ρ can be directly calculated using (14) as the SQI.

A performance evaluation of the SQI defined in (14) was presented in [15] with respect to physically simulated motion and respiratory noise. Statistics of ρ may need to be established for healthy and patient populations with different CVD to minimize false positive rate during detection of noisy BCG recordings. When repetitive measurements are not feasible, statistics of ρ can be obtained using the synthesis algorithm (Fig. 2) with a unity noise gain. Using the proposed BCG sub- template synthesis algorithm, we evaluate the impact of noise gain on the average correlation coefficient in Section VI-G.

VI. Human Subject Experiments

In this section, the template-based modeling and synthesis algorithm is tested with experimental results based on data collected from 13 healthy subjects. Morphological changes on the sub-template and parent template BCG heartbeat are shown for various additive noise levels. The SQI is investigated with respect to increasing noise level using the developed modeling and synthesis approach. Receiver operating characteristics (ROC) curves are also obtained at various noise levels for the detection of noisy BCG recordings as an example use of this work.

A. Experimental Setup

In the experiments, BCG and ECG signals were simultaneously recorded. The BCG signal was recorded using a force plate for healthy subjects. The details of the instrumentation can be found for the force plate in [17]. Three ECG gel electrodes were connected in the Lead II configuration on healthy subjects (see Fig. 1(a)). Subjects were asked to stand still on the force plate for 60sec. Written informed consent was obtained from subjects, and the protocol was approved by the Georgia Institute of Technology (protocol H13512) Institutional

Review Board (IRB). A total of 13 subjects were used for this study (average age of 27.5 ± 5.8years, weight of 74.8 ± 13.6kg, and height of 174.8 ± 10.1cm; 10 males, and 3 females). BCG and ECG signals were bandpass filtered with a passband of 0.8–20Hz and 1–40Hz, respectively [23], [24]. To divide the recorded BCG signal into heartbeats for each RR interval, the ECG R-peaks were detected using a threshold-based peak detection algorithm.

B. Distribution of Sub-Template Noise

In Fig. 3, histograms of the sub-template noise level are presented. Noise level in sub-template BCG heartbeats was calculated using (9) for 6-beat averaged BCG heartbeats using only the measured data from 13 healthy subjects. For the histogram in Fig. 3(a), each noise level in a sub-template was standardized using its mean and variance, and a histogram was created using the data from all subjects. A normal distribution was fit to the histogram and is shown on the same figure. For the histogram in Fig. 3(b), each point in the sub-template noise vector is grouped across the sub-template noise vectors from the same subject. Then, each group was standardized based on its subject-specific mean and variance, and a histogram was created using all of the population data. The fitted normal distribution is shown on the same plot as well. In Fig. 3(c), histograms are plotted separately for each subject after each point in the sub-template noise vectors was grouped and standardized across sub-templates of corresponding subject. The same normal distribution fitted for Fig. 3(b) was also plotted.

The histograms obtained based on different computations for noise level in sub-templates exhibit a similar shape to the standard normal distribution (the mean and the standard deviation of the fitted normal distributions are approximately 0 and 1, respectively). These results show that there is a good fit between the normal distribution and the histogram of sub-template noise based on the data obtained from the human subject experiments. Accordingly, sub-template noise levels can be reasonably modeled using estimated statistics in (10) and (11), and a normally distributed random vector.

C. Synthesized Sub-Template BCG Heartbeats

To illustrate the synthesized sub-template BCG heartbeats using the devised algorithm (Fig. 2), we compare the morphology of synthesized sub-template BCG heartbeats for various noise gains to the measured ones. The number of heartbeats, W, for the sub-template estimation was set as a constant 6 beats. Since both healthy heart rate and healthy respiration rate are wide intervals (60–100 beats per minute for healthy heart rate and 12–20 breaths per minute for healthy respiration rate), one can typically get 3 to 8 heartbeats per breathing cycle. Data recording from a subject was used for the illustration of an instance of the synthesized BCG heartbeats in Fig. 4.

Morphology of the measured sub-template BCG heartbeats is presented in Fig. 4(a). To synthesize sub-template BCG heartbeats, the algorithm presented in Section V-A (Fig. 2) is applied to recorded BCG heartbeats. The noise statistics were calculated for sub-templates, and accordingly the synthetic noise is added to the sub-template BCG heartbeats rather than individual heartbeats. In Fig. 4(b), synthesized sub-template BCG heartbeats with a noise gain of 1 are presented.

Finally, sub-template BCG heartbeats with a noise gain of 10 are presented in Fig. 4(c). Due to an increased noise component on the sub-template heartbeats, the J-wave morphology was further distorted. Such distortion may hamper the ability to distinguish the peak of the J-wave from the rest of the BCG heartbeat, and reliability of the estimated parameters (e.g., RJ interval) could be reduced.

D. Synthesized Parent Template BCG Heartbeats

Continuing with the study of the morphology of the synthesized parent template BCG heartbeat, in Fig. 4(d), parent template BCG heartbeats are presented. The measured parent template BCG heartbeat is compared with the synthesized parent template BCG heartbeats with noise gains of 1, 10, and 20. It is observed that when the sub-templates are averaged to calculate the parent template, the noise effects may be cancelled out. However, the J-wave morphology is still distorted and difficult to distinguish as the noise level increases for both subjects. Hence, the estimated parameters, such as timing and amplitude of the J-peak would likewise be altered, and ultimately the accuracy of J-peak detection algorithms would be compromised.

E. Convergence of the Average Correlation Coefficient and BCG Measurement Length for Parent Template Estimation

In Fig. 5, the average correlation coefficient of cumulatively averaged BCG heartbeats to the parent template BCG heartbeat is shown for 13 subjects. The linear correlation between the cumulative average of BCG heartbeats to parent template reaches approximately 1, after more than 40 heartbeats are included in the cumulative average. When the number of heartbeats included in the cumulative average is 5 or greater, the correlation coefficient increases with a slower rate, however, eventually converges to 1. Therefore, addition of more heartbeats to the cumulative average provides small improvement for the estimation of the parent template. This saturation in the average correlation coefficient supports the conjecture that to estimate the parent template BCG heartbeat reliably, there should be at least 40 heartbeats in the BCG recording (Fig. 5).

F. Distribution of Correlation Coefficient and Memoryless Property of Sub-Templates

To study the distribution of the correlation coefficient between the parent template and a sub-template, ξ is defined as 1 - the correlation coefficient between the parent template and a sub-template. To obtain the histogram, ξ was computed using measurements from 13 healthy subjects, and was standardized for each subject. In addition, the probability density function of the exponential distribution with a mean of 0.08 is also presented alongside the histogram in Fig. 6. This result shows that ξ can be modeled using the exponential distribution when the subject is at rest. The mean of the distribution may depend on subject-dependent variances in the cardiopulmonary system (both cardiac-cycle and breathing-cycle). Moreover, the sample mean, e.g., averaging performed in (14), is the unbiased maximum likelihood estimator for the mean of the exponential distribution.

Changes in the cardiovascular system during measurement and motion artifacts may also affect the value of the ξ. However, the fit between the histogram of ξ and exponential distribution points out the memoryless property of the correlation coefficient such that, if the

ξ is conditioned having a specific earlier value, the distribution of ξ is the same as the original unconditional distribution when the subject is at rest.

G. Noise Analysis based on Average Correlation Coefficient

Here, we investigate the average correlation coefficient between sub-templates and the parent template with respect to the additive noise gain in a subject-by-subject manner. The synthesis algorithm presented in Section V-A was used to create BCG heartbeats distorted by noise. The BCG SQI as described in Section V-B (average sub-template correlation to parent template) was used for quantification of the distortion in the estimated BCG parent template. The parent template BCG heartbeat is estimated for each of the synthesized BCG sub-templates of each subject based on the adjusted noise level, and then the correlation coefficient was calculated for the corresponding noise level. Therefore, results only depend on the personal statistics without requiring any prior measurement. Simulations were performed at different cycle lengths (6 and 12 heartbeats). Since the synthesis algorithm uses random number generation for the RJ interval and additive noise, simulations were repeated 100 times for each noise level, each cycle length, and each person. Then, the average correlation coefficient is calculated along with the standard deviation.

In Fig. 7, noise analysis results are presented based on experiments with 13 subjects. For the original measurements, the average correlation coefficient is represented with a noise gain equal to 0. For the original measurements case, there are no error bars in the plots, since these correlation coefficients were obtained using measured data. When the noise gain is equal to 1, the average correlation coefficient of synthesized templates may increase compared to the average correlation of measured templates. This is due to the fact that the synthesized sub-templates can be smoother than the measured sub-templates, since they are generated based on the same parent template for each person. The smoothening feature of the synthesis algorithm can also be observed comparing the measured sub-templates in Fig. 4(a) and the synthesized sub-templates in Fig. 4(b). As noise gain is increased from 1 to 50, the average correlation coefficient is observed to be strictly decreasing for all subjects in Fig. 7.

When fewer beats are used to generate a sub-template, increasing the noise gain has a stronger adverse effect on the signal. This trend can be seen by the faster rate of reduction of the average correlation coefficient (BCG SQI) with fewer heartbeats. Moreover, the variance of the average correlation coefficient increases as the noise gain is increased for all sub-template sizes.

H. Application to Detection of Noisy BCG Measurements

Here, we, first, study the ROC curves for the detection of the noisy BCG signals using the proposed BCG SQI in Section V-B. To calculate the ROC curves, we define decision variable θ as $\theta = 1-\rho$. As the noise level increases, the BCG signal is expected to have a lower ρ, and hence, higher θ. Detection of noisy BCG signals is a statistical hypothesis testing problem, with the null $\mathscr{H}_0$ and alternative $\mathscr{H}_1$ hypotheses as

$$\mathcal{H}_0: \text{Usable BCG Measurement} \quad (15)$$
$$\mathcal{H}_1: \text{Noisy BCG Measurement}$$

and the decision rule is given by

$$\theta \underset{\mathcal{H}_0}{\overset{\mathcal{H}_1}{\gtrless}} \gamma, \quad (16)$$

where γ is the decision threshold.

1) Calculation of ROC Curves: P_D and P_F are calculated below to show example use of the proposed modeling, synthesis, and noise analysis framework. The probability of false alarm (false positive) is defined as [22]

$$P_F = \int_{\gamma}^{\infty} P(\theta|\mathcal{H}_0). \quad (17)$$

The probability of detection (true positive) is defined as [22]

$$P_D = \int_{\gamma}^{\infty} P(\theta|\mathcal{H}_1). \quad (18)$$

SQI calculation uses the average correlation coefficient in a recording instead of an individual correlation coefficient.

The average correlation coefficient is the linear addition of individual correlation coefficients and subsequent division by a scalar. By the law of large numbers, when these individual correlation coefficients are added, the sum divided by a scalar (the distribution of the sample mean) is expected to converge to a Gaussian distribution. Therefore, we assume θ is Gaussian distributed to study ROC curves. Given the false alarm probability, the decision threshold, γ, is obtained by

$$\gamma = E\{\theta|\mathcal{H}_0\} + \sqrt{\text{Var}(\theta|\mathcal{H}_0)}\mathcal{Q}^{-1}(P_F), \quad (19)$$

where $\mathcal{Q}$ is the Q-function. $E\{\theta|\mathcal{H}_0\}$ and $\text{Var}(\theta|\mathcal{H}_0)$ are calculated using the synthesis algorithm (Fig. 2) with a noise gain of 1. Using (18) and (19), the probability of detection is calculated as

$$P_D = 1 - \mathcal{Q}\left(\frac{\gamma - E\{\theta|\mathcal{H}_1\}}{\sqrt{\mathrm{Var}\{\theta|\mathcal{H}_1\}}}\right), \quad (20)$$

where $E\{\theta|\mathcal{H}_1\}$ and $\mathrm{Var}(\theta|\mathcal{H}_1)$ are calculated using the synthesis algorithm (Fig. 2) with various noise gains from 5 to 40. To obtain Fig 8, P_F values were swept from 0 to 1 in (19) to obtain decision threshold γ for each P_F. Then, the corresponding P_D value for each P_F was calculated using (20).

2) Detection of Noisy Recordings: In Fig. 8(a) and (b), we evaluate the probability of detection (P_D) of a noisy recording with respect to the probability of a false alarm for different sub-template sizes of 6-beat and 12-beat, respectively. For the sub-templates made of 6 heartbeats, the detection probabilities are higher for the same false alarm probability compared to the sub-templates made of 12 heartbeats. This points out that lower cycle length selection leads to better noisy recording detection performance. As the noise gain increases from 5 to 40, the detection probability also increases. Accordingly, the proposed BCG SQI based on average correlation coefficient can be useful to distinguish noisy BCG measurements.

Additionally, through experimental studies in [15], we showed that the proposed SQI provides statistically significant distinguishability ($p < 0.01$) for the BCG recordings where noise was physically simulated for motion artifacts, and physiological variation (speaking and deep breathing), i.e., $\mathbf{w}_{\text{ext}}$ and $\mathbf{w}_{\text{phy}}$, respectively, in (4).

I. Discussion

Outside-of-clinic monitoring of cardiovascular health and performance can enable preventative care, improve continuity of care for patients with chronic health conditions such as heart failure, and allow personalized adjustment of care based on patient state [1], [2]. A major challenge in home monitoring of cardiovascular health using any non-invasive technology is the reliability of the measured signals (it is not obvious from a measurement which components are “signal” and which are “noise”). Thus, the proposed modeling, synthesis, and noise analysis framework aims to provide a computational prototype toward mitigating the potential errors in the health parameters and patient state information derived from the BCG recordings.

1) Main Results:

We outlined a novel statistical methodology that addresses signal modeling, synthesis, and noise analysis for BCG signals obtained on a modified weighing scale platform and given ECG R-peaks. Distinctive results of our work are summarized below.

- We have outlined a framework based on subject-specific statistics, which can be used to quantify the noisiness of a person’s BCG recording automatically without requiring any *a priori* information regarding the person’s BCG and ECG signals or health (Section III, IV, and V).

- We have provided a data-driven determination of the minimum number of heartbeats required to perform template-based statistical modeling of a BCG recording (Fig. 5).
- Using a synthetic model for BCG heartbeat, we showed matched filtering can be used to detect the distortion in the BCG signal due to noise (Fig. 7).

2) Applications:

Our proposed statistical model and synthesis algorithm for cycle-averaged BCG heartbeats takes into consideration the periodic nature of the cardiopulmonary system, such as the periodicity of heartbeats and breathing, and provides an opportunity for assessment of noise in the BCG signals. Two unique aspects of our work are that it does not depend on population-wide training, and it provides subject-specific modeling that facilitates personalized noise assessment.

In addition, quantification of the noise (the difference between sub-templates and the parent template) could be useful to evaluate differences caused by respiration on the BCG signal. The physiological reasoning behind this is that several parameters of cardiovascular mechanics are modulated by breathing due to the changes associated with inhalation/exhalation [18]–[20]. Accordingly, the BCG morphology is also expected to change. We studied the effects of respiration (specifically, via speaking and deep breathing) on BCG signal in more detail in [15].

Using the synthesis algorithm we proposed, we obtained the statistics for true and false detection of noisy BCG recordings in Fig. 8. The developed synthesis algorithm provided an opportunity to create multiple realizations of the BCG response from the same subject. We only used one measurement from each subject, and applied our synthesis algorithm. Then, we obtained ROC curves for each subject, and averaged ROC curves over the population for the compactness of presentation. Our modeling and synthesis framework was useful to obtain those plots.

3) Constraints:

The proposed methodology assumes that the subject is at rest, such that heart rate remains quite stable (the subject remains in a steady-state condition). This constraint is in line with the scenario of longitudinal monitoring of the clinical state of patients with heart failure outside of the clinic. Each individual BCG recording can be taken daily in uncontrolled settings at home while the patient is standing still and at rest, and a relatively stable heart rate can be expected. The changes in BCG signals can then be tracked across many such recordings, each of which are taken with stable heart rate. For the computation of the SQI, equal weight is given to each correlation coefficient in (14) under the assumption that the subject is at rest. When there exists an established memory model for the correlation coefficient between the sub-templates and the parent template, use of equal weighting could provide inferior performance compared to the use of optimal weights for combination (for example, with respect to physical activity and exercise recovery).

4) Future Work:

Adjustable noise gain in the synthesis algorithm can be extended by a coloring transformation to reflect the desired correlation property for additive noise. A more detailed description of the noise characteristics can be incorporated by the covariance matrix which can be estimated by repetitive testing from the same subject under multiple noisy scenarios (e.g., motion, speaking, changes in autonomic state, etc.). In future work, estimation of the correlation matrix for the sub-template BCG heartbeats can be studied to obtain detailed statistics of the additive noise, which would require longer duration and repeated measurements for characterization.

While our modeling and synthesis framework was useful to obtain ROC curves in Fig. 8, there is a need for evaluation over a larger set of recordings with manually annotated noisy and usable recordings, which is an important step for future work. The average correlation coefficient (sample mean of the linear correlation coefficient) can be modeled reasonably by a Gaussian distribution. Additionally, the distribution for the true detection in (20) can be tuned for the targeted specific noisy scenarios according to subject-specific correlation coefficient statistics after repetitive testing with each individual subject.

At this stage, we only target scenarios where the subject remains in a steady-state condition, which can have strong clinical relevance. Our work may be extended to exercise recovery by applying multiple parent templates, however, this would require further data collection from the same subjects for reliable template estimation and increase the complexity.

VII. Conclusion

Long-term monitoring of the cardiovascular systems outside of clinical settings is important for assessing wellness and may provide progress towards personalized medicine. In this paper, a cycle-averaged statistical model is proposed for BCG heartbeats incorporating individualized statistics. A template-based synthesis algorithm is presented where the additive noise element can be adjusted to reflect any correlation relation in and inter BCG heartbeats. To utilize the proposed modeling and synthesis approach, no side information (any prior knowledge) on the BCG signal is required. Finally, a metric for BCG signal quality assessment is proposed, and the impact of noise level is evaluated using the data obtained from experiments. The developed framework can be used to assess the effectiveness of BCG signal processing algorithms, e.g., probabilities of mis-detection and overall false-alarm rates can be characterized with respect to various additive noise levels.

Acknowledgments

This work was supported by the National Institutes of Health (NIH), National Heart, Lung and Blood Institute, under Grant R01HL130619. The content is solely the responsibility of the authors and does not necessarily represent the official views of the NIH.

Biography

A. Ozan Bicen (S'08, M'17) obtained his Ph.D. degree in electrical and computer engineering from the Georgia Institute of Technology, Atlanta, GA in 2016. He is currently a postdoctoral researcher at the Georgia Institute of Technology. His research interests include physiological sensing, statistical signal processing, biomedical instrumentation, and communication systems.

Daniel C. Whittingslow received his B.S. degree in biomedical engineering from Georgia Tech Atlanta, GA in 2013. He then began the MD/PhD program at Emory University and Georgia Tech. His research focuses on developing devices for monitoring of health conditions. He is heavily involved in connecting clinicians and engineers.

Omer T. Inan (S'06, M'09, SM'15) received the B.S., M.S., and Ph.D. degrees in electrical engineering from Stanford University in 2004, 2005, and 2009, respectively. He is currently an Associate Professor of Electrical and Computer Engineering at the Georgia Institute of Technology. His research focuses on non-invasive physiologic sensing and modulation.

References

[1]. Bui AL, and Fonarow GC, "Home Monitoring for Heart Failure Management," J. Am. Coll. Cariol, vol. 59, no. 2, pp. 97–104, 2012.

[2]. Pare G, Jaana M, and Sicotte C, "Systematic Review of Home Telemonitoring for Chronic Diseases: The Evidence Base," Journal of the American Medical Informatics Association, vol. 14, no. 3, pp. 269–277, 2007. [PubMed: 17329725]

[3]. Starr I, Rawson AJ, Schroeder HA, and Joseph NR, "Studies on the Estimation of Cardiac Output in Man, and of Abnormalities in Cardiac Function, from the Heart's Recoil and the Blood's Impacts; the Ballistocardiogram," Amer. J. Physiol, vol. 127, pp. 1–28, 1939.

[4]. Starr I, and Schroeder HA, "Ballistocardiogram. II. Normal Standards, Abnormalities Commonly Found in Diseases of the Heart and Circulation, and Their Significance," vol. 19, no. 3, pp. 437–450, 1940.

[5]. Starr I and Wood F, "Twenty-year Studies with the Ballistocardiograph: the Relation between the Amplitude of the First Record of Healthy Adults and Eventual Mortality and Morbidity from Heart Disease," Circulation, vol. 23, no. 5, pp. 714–732, 1961.

[6]. Mandelbaum H and Mandelbaum R, "Studies Utilizing the Portable Electromagnetic Ballistocardiograph: IV. The Clinical Significance of Serial Ballistocardiograms Following Acute Myocardial Infarction," Circulation, vol. 7, no. 6, pp. 910–915, 1953. [PubMed: 13051833]

[7]. Inan OT, Park D, Giovangrandi L, Kovacs GTA, "Noninvasive Measurement of Physiological Signals on a Modified Home Bathroom Scale," IEEE Transactions on Biomedical Engineering, vol. 59, no. 8, pp. 2137–2143, 2012. [PubMed: 22318479]

[8]. Gonzalez-Landaeta R, Casas O, and Pallas-Areny R, "Heart Rate Detection from an Electronic Weighing Scale," IOP Physiological Measurement, vol. 29, no. 8, pp. 979–988, 2008.

[9]. Gilaberte S, Gomez-Clapers J, Casanella R, and Pallas-Areny R, "Heart and Respiratory Rate Detection on a Bathroom Scale Based on the Ballistocardiogram and the Continuous Wavelet Transform," in Proc. IEEE EMBC, Buenos Aires, Argentina, 2010.

[10]. Shin JH, Lee KM, and Park KS, "Non-constrained Monitoring of Systolic Blood Pressure on a Weighing Scale," IOP Physiological Measurement, vol. 30, no. 7, pp. 679–693, 2009.

[11]. Chung EK, Electrocardiography: Practical Applications with Vectorial Principles, 3rd ed. Norwalk, CT: Appleton-Century-Crofts, 1985.

[12]. Inan OT, Migeotte P-F, Park K-S, Etemadi M, Tavakolian K, Casanella R, Zanetti J, Tank J, Funtova I, Prisk K, Di Rienzo M, "Ballistocardiography and Seismocardiography: A Review of Recent Advances," IEEE Journal of Biomedical and Health Informatics, vol. 19, no. 4, pp. 1414–1427, 2015. [PubMed: 25312966]

[13]. Parlikar TA, Heldt T, and Verghese GC, "Cycle-Averaged Models of Cardiovascular Dynamics," IEEE Transactions on Circuits and Systems–I: Regular Papers, vol. 53, no. 11, pp. 2459–2468, 2006.

[14]. Kim C-S, Ober SL, McMurtry MS, Finegan BA, Inan OT, Mukkamala R, and Hahn J-O, "Ballistocardiogram: Mechanism and Potential for Unobtrusive Cardiovascular Health Monitoring," Scientific Reports, vol. 6, article no: 31297, 2016.

[15]. Bicen AO, and Inan OT, "A Signal Quality Index for Ballistocardiogram Recordings based on Electrocardiogram RR Intervals and Matched Filtering," in Proc. the IEEE International Conference on Biomedical and Health Informatics (BHI) 2018, Las Vegas, NV, 2018.

[16]. Etemadi M, Inan OT, Giovangrandi L, Kovacs GTA, "Rapid Assessment of Cardiac Contractility on a Home Bathroom Scale," IEEE Transactions on Information Technology in Biomedicine, vol. 15, no. 6, pp. 864–869, 2011. [PubMed: 21843998]

[17]. Bicen AO, Gurel NZ, Dorier A, and Inan OT, "Improved Pre-Ejection Period Estimation from Ballistocardiogram and Electrocardiogram Signals by Fusing Multiple Timing Interval Features," IEEE Sensors Journal, vol. 17, no. 13, pp. 4172–4180, 2017.

[18]. Lilly LS, Pathophysiology of Heart Disease: A Collaborative Project of Medical Students and Faculty, 6th ed. Philadelphia, PA: Lippincott Williams & Wilkins, 2015.

[19]. Stein PK, S Bosner M, Kleiger RE, and Conger BM, "Heart Rate Variability: a Measure of Cardiac Autonomic Tone," American Heart Journal, vol.127, no. 5, pp.1376–1381, 1994. [PubMed: 8172068]

[20]. Zaniboni M, Pollard AE, Yang L, and Spitzer KW, "Beat-to-beat Repolarization Variability in Ventricular Myocytes and Its Suppression by Electrical Coupling," American Journal of Physiology - Heart and Circulatory Physiology, vol. 278, no. 3, pp. H677–H687, 2000. [PubMed: 10710334]

[21]. Klabunde RE, Cardiovascular Physiology Concepts, 2nd ed. Lippincott Williams & Wilkins, 2011.

[22]. Van Trees HL, Detection, Estimation, and Modulation Theory, Part I New York: John Wiley & Sons, 1968.

[23]. Gomez-Clapers J, Serra-Rocamora A, Casanella R, and Pallas-Areny R, "Uncertainty Factors in Time-interval Measurements in Ballisto-cardiography," in Proc. 19th IMEKO TC-4 Symp. 17th IWADC Workshop Adv. Instrum. Sens. Interoperability, pp. 395–399, Barcelona, Spain, 2013.

[24]. Sornmo L, and Laguna P, Bioelectrical Signal Processing in Cardiac and Neurological Applications, 1st ed. Academic Press, 2005.

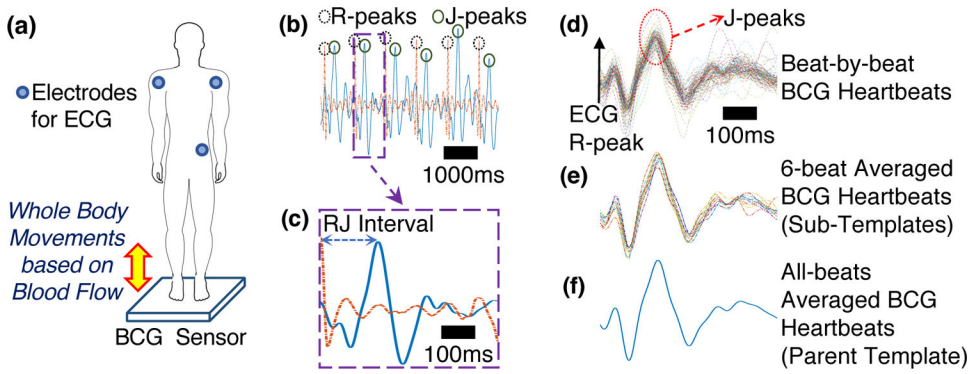

Fig. 1.

Placement of BCG and ECG sensors on a human subject (a) (to adapt this system for home use, a modified weighing scale could be used as BCG sensor, and the ECG gel electrodes could be replaced with handlebar electrodes). Traces of synchronized ECG and BCG measurements in (b), and RJ interval for a single BCG heartbeat in (c) (amplitudes of signals are scaled for ease of demonstration). BCG responses: beat-by-beat (d), 6-beat averaged (sub-templates) (e), and all-beats averaged (parent template) (f).

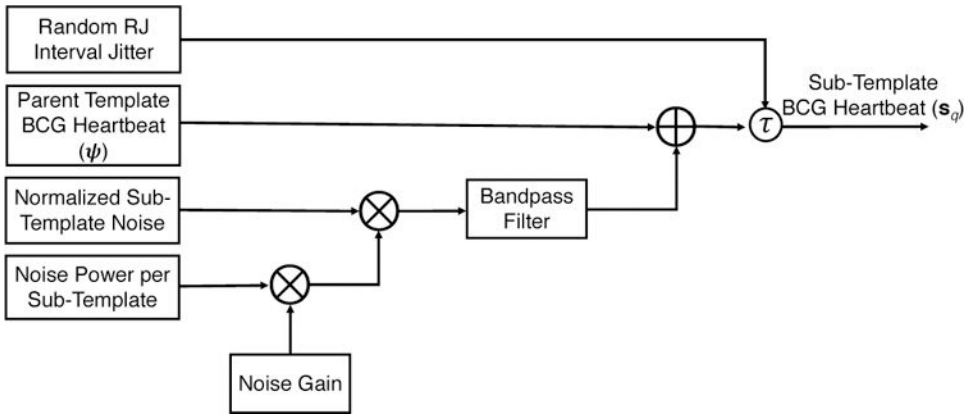

Fig. 2.

Synthesis of sub-template BCG heartbeats with synthetic additive noise and RJ interval jitter.

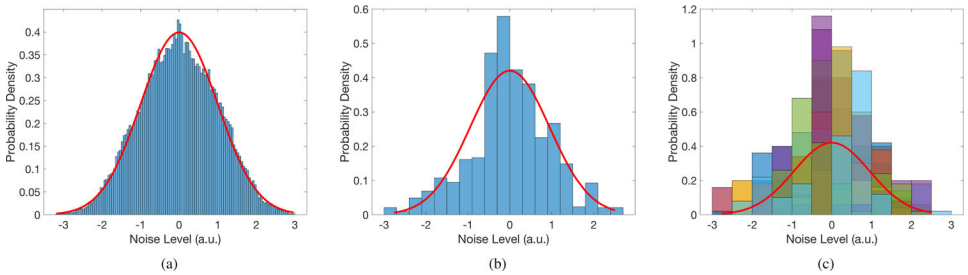

Fig. 3.

Histograms of noise level in the sub-template BCG heartbeats based on measured data from 13 subjects, and the fitted normal distribution is shown with a solid red line. In (a), each sub-template was standardized, and histogram was created using the all population data. In (b), for each subject, each point in the sub-templates was standardized across sub-templates of the corresponding subject, and the histogram was created using all of the population data. In (c), histograms are plotted separately for each subject after each point in the sub-templates was standardized across sub-templates of the corresponding subject.

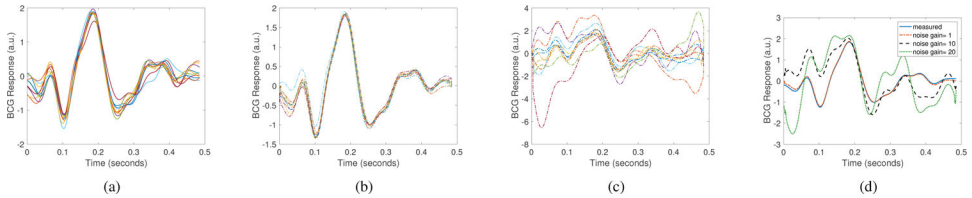

Fig. 4.

Morphology of sub-template and parent template BCG heartbeats. These results were obtained based on measurements from a healthy subject. Measured sub-template BCG heartbeats in (a). Instances of the synthesized sub-template BCG heartbeats with unity noise gain (b). Instances of the synthesized sub-template BCG heartbeats with noise gain of 10 in (c). Comparison of the measured parent template BCG with synthesized instances of parent template BCG heartbeat for various noise gains in (d).

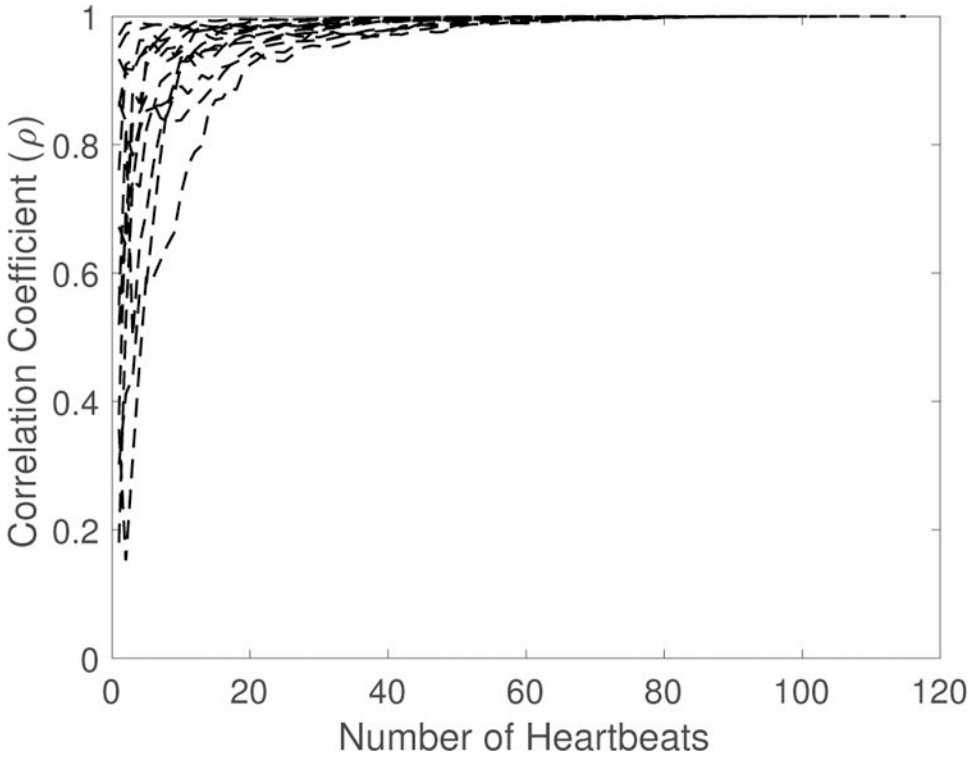

Fig. 5.

Convergence of the correlation coefficient between the cumulatively averaged BCG heartbeat and parent template BCG heartbeat with respect to number of heartbeats in the cumulative average for 13 subjects (each line represents one subject).

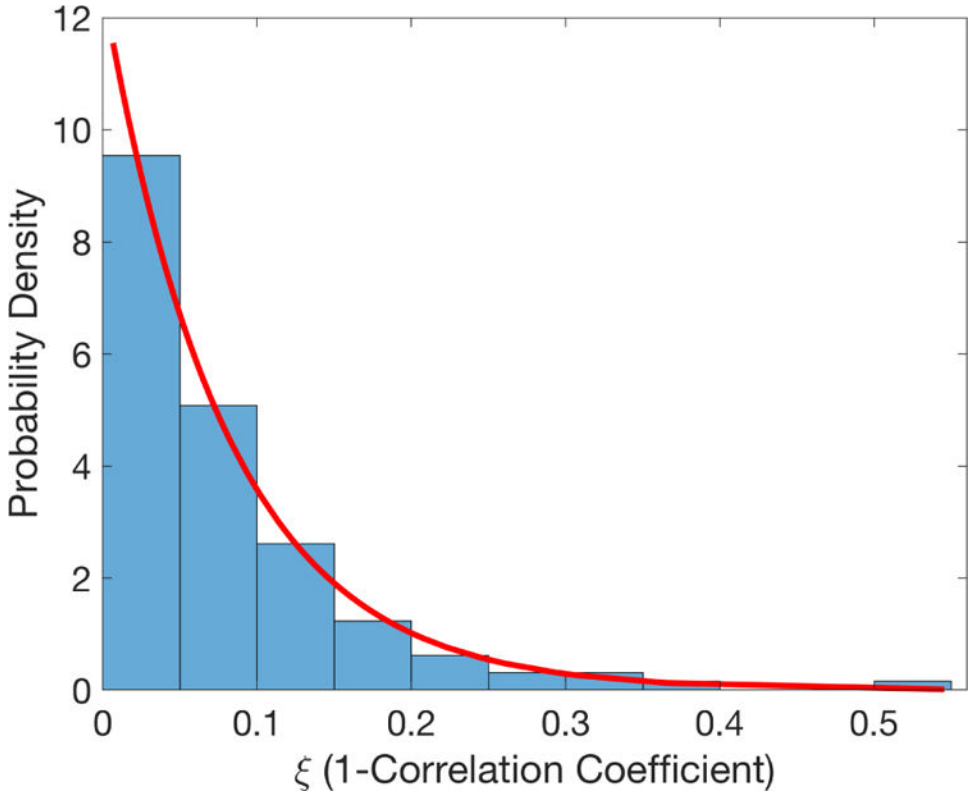

Fig. 6.

Histogram of ξ (1-linear correlation coefficient between the parent template and a sub-template) based on measured data from 13 subjects. The exponential distribution with a mean of 0.08 is shown with red dashed lines.

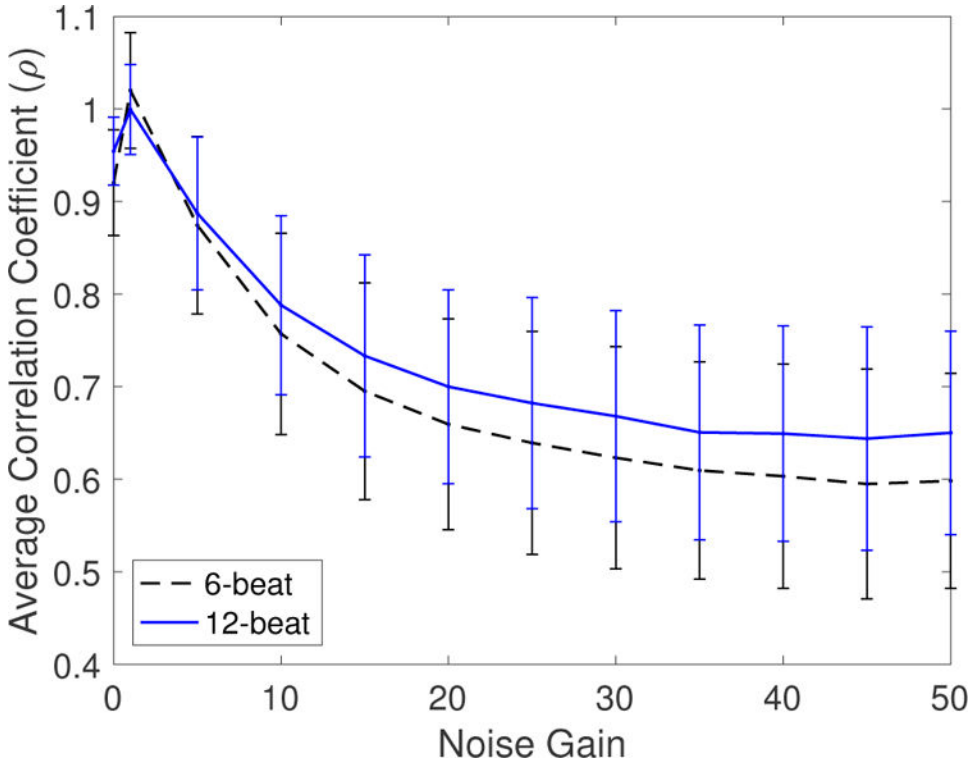

Fig. 7.

The average correlation coefficient (ρ) is presented with respect to the increasing noise gain based on experiments with 13 healthy subjects. Sub-templates composed of 6 and 12 heartbeats are used. Noise gain equal to 0 represents the average correlation coefficient for the original measurement. For noise gain equal to 1 to 50, ρ for each subject was normalized with respect to the original measurement value. Then, mean across the population was presented with error bars presenting the standard deviation.

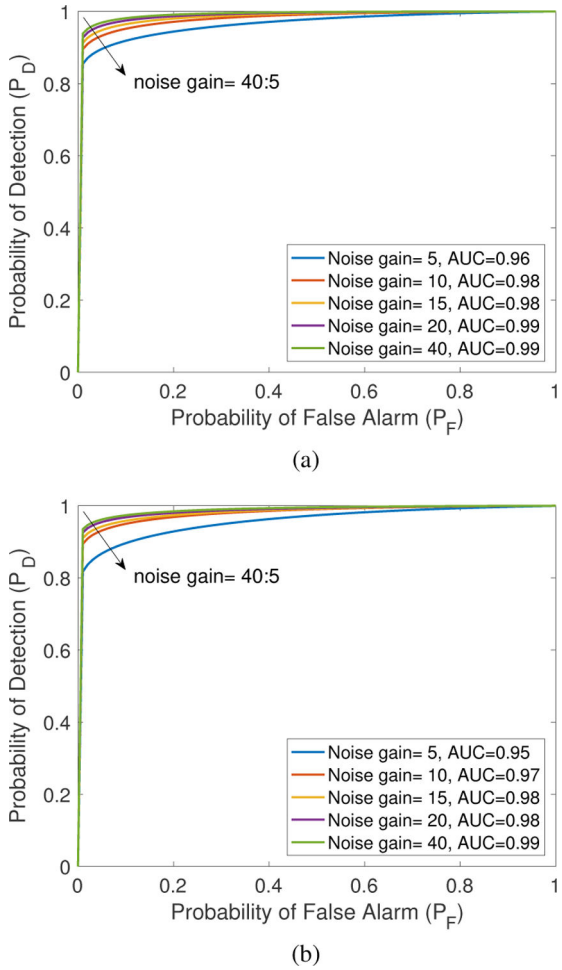

Fig. 8.

ROC curves for healthy subjects in (a) and (b), where sub-templates were made of 6 and 12 BCG heartbeats, respectively. ROC curves were obtained for each subject at each noise level separately, and then averaged across the population for compactness of presentation. The area under the receiver operating characteristics curve (AUC) is given in the legend for each noise level.